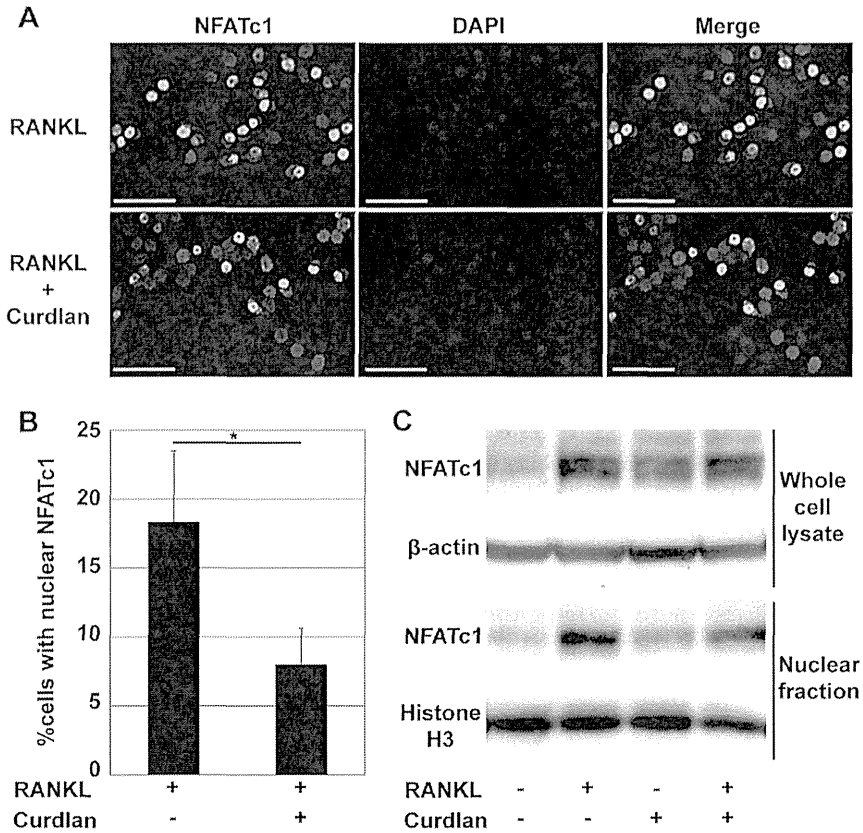

FIGURE 9. **Effect of curdlan on RANKL-stimulated NFATc1 activity d-RAWs.** d-RAWs were incubated with or without curdlan (25 μg/ml) in the presence of RANKL (40 ng/ml) for 3 h. *A*, cells were fixed, permeabilized, and stained for NFATc1 (*green*) and nuclei (*blue*). *Scale bars* = 50 μm. *B*, cells showing nuclear translocation of NFATc1 protein were scored. Data show the percentage of nuclear NFATc1 positive cells from three independent samples, and *error bars* represent mean ± S.D. Data were analyzed by Student's *t* test. *, $p < 0.05$ in comparison with treatment with RANKL. *C*, d-RAWs (2×10^6 cells) were incubated with or without curdlan (25 μg/ml) in the presence of RANKL (40 ng/ml) for 6 h. Whole cell lysates or nuclear fractions were prepared and analyzed by Western blotting, with the blots probed for NFATc1. Equal sample loading and purity of nuclear fractions were controlled by analyzing β-actin and histone H3.

modern conditional gene targeting and transgenic technologies, the field of combined bone and immunology, known as osteoimmunology, is advancing rapidly. Previous studies have reported the existence of a specific β-glucan receptor, dectin 1, on effector cells, including macrophages (36–38). This receptor binding process is thought to be the first step in mediating the activating immunomodulatory effects of β-glucans.

Osteoclasts are derived from myeloid progenitors, which also give rise to monocytes, macrophages, and dendritic cells. The direct effects of β-glucan on osteoclastogenesis have not been investigated to date. In this study, we used curdlan, a linear β-1,3 glucan from the bacterium *Alcaligenes faecalis*, as a dectin 1-specific agonist (39–42). Interestingly, osteoclast formation of BMCs, induced by M-CSF and RANKL, was decreased by addition of curdlan (Fig. 1, *A* and *B*), indicating that curdlan has a protective effects against osteoclastogenesis. This effect appears not to be due to the toxicity of curdlan because curdlan treatment did not significantly alter the proliferation of BMCs compared with M-CSF and RANKL (data not shown).

Bone resorption is a multistep process initiated by the proliferation of immature osteoclast precursors. This is followed by commitment of these cells to the osteoclast phenotype and degradation of the organic and inorganic phases of bone by mature resorptive cells. When cultured with bone or dentin, osteoclasts excavate resorptive lacunae, or pits, that are similar to the structures formed when cells degrade bone *in vivo*. Furthermore, the size of the resorption lacunae formed *in vitro* is used as a quantitative measure of osteoclast activity (43). In this study, we used an Osteo Assay Stripwell Plate® coated with a calcium phosphate substrate and observed the down-regulation of the pit-forming activity of osteoclasts stimulated with M-CSF and RANKL (Fig. 1, *C* and *D*). In addition, actin cytoskeletal organization includes the ruffled membranes and the actin ring or sealing zone, which is essential for mature osteoclasts to perform bone resorption (27, 28, 44, 45). Curdlan treatment showed impaired actin cytoskeletal organization in BMCs, suggesting that curdlan is involved in the regulation of actin ring formation induced by M-CSF and RANKL (Fig. 1*E*).

The cell specificity of dectin 1 expression suggested that the antiosteoclastogenic effect of curdlan was mainly dependent on osteoclast precursors, not osteoblast/stromal cells (Fig. 2). We used a homogeneous clonal population of murine monocyte RAW 264.7 cells to elucidate the direct effects of RANKL and curdlan on osteoclast differentiation and function. This cell line is known to express RANK and differentiate into TRAP-positive cells when cultured with bone slices and RANKL (46). The main advantage of this system is that it does not contain any osteoblast/bone marrow stromal cells, which may also be tar-

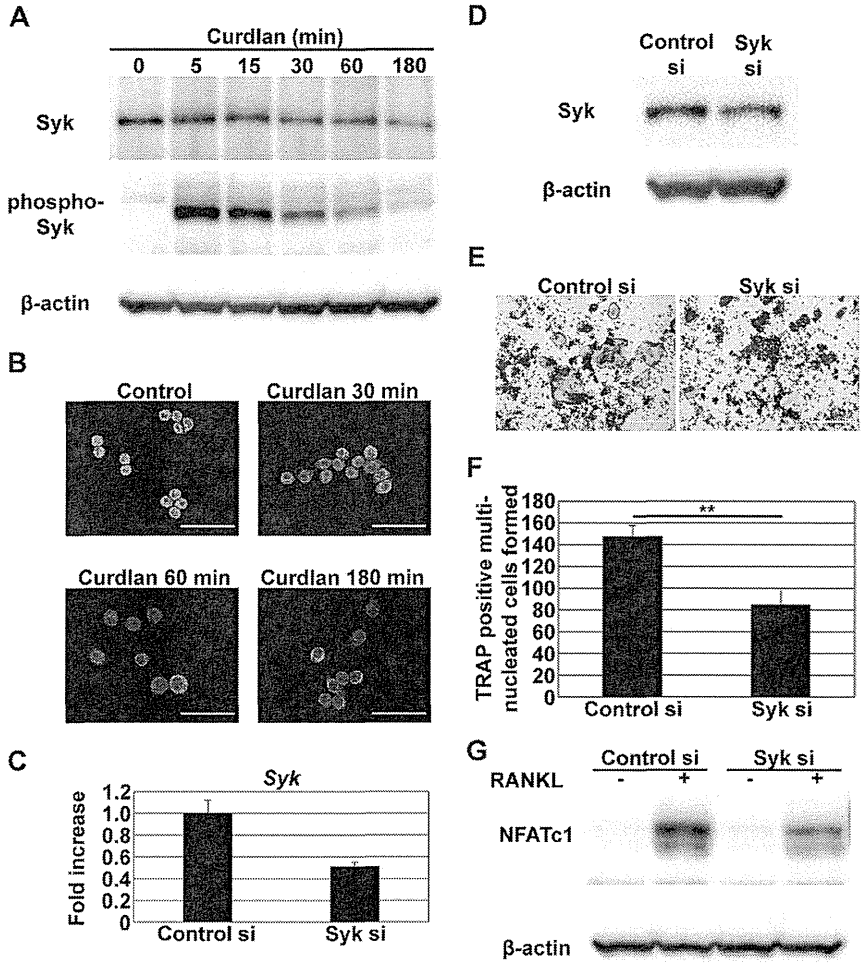

FIGURE 10. **Effect of silencing Syk on RANKL-induced osteoclastogenesis in d-RAWs.** d-RAWs were incubated with or without curdlan (25 μg/ml) for the indicated time. *A*, whole cell lysates were subjected to SDS-PAGE and Western blotting analyses, with the blots pro bed for Syk and phosphorylated Syk. Equivalent protein aliquots of cell lysates were also analyzed for β-actin. *B*, cells were fixed, permeabilized, and stained for Syk (*green*) and nuclei (*blue*). *Scale bars* = 100 μm. d-RAWs were transfected as labeled in *C–G* with either control or Syk-specific siRNAs (*si*). *C*, total RNA was isolated from the transfected cells and reverse-transcribed into cDNA, and then PCR amplification was performed using primers specific for Syk and Gapdh. Data show the fold changes in Syk mRNA copy number values from three independent samples, and *error bars* represent mean ± S.D. After transfection, cells were incubated in the presence of RANKL (40 ng/ml) for 7 days. *D*, whole cell lysates were isolated from the transfected cells and subjected to SDS-PAGE and Western blotting analyses, with the blots probed for Syk. Equivalent protein aliquots of cell lysates were also analyzed for β-actin. *E*, cells were stained for TRAP activity. *Scale bars* = 500 μm. *F*, the number of osteoclasts differentiated from transfected d-RAWs was counted after staining for TRAP activity. Data show the number of osteoclasts from three independent samples, and *error bars* represent mean ± S.D. Data were analyzed by Dunnett's test after one-way ANOVA. **, $p < 0.01$ in comparison with d-RAWs transfected control siRNA. *G*, transfected d-RAWs were incubated in the presence or absence of RANKL (40 ng/ml) for 72 h. Whole cell lysates were subjected to SDS-PAGE and Western blot analyses, with the blots probed for NFATc1. Equivalent protein aliquots of cell lysates were also analyzed for β-actin.

gets of RANKL and curdlan actions. We also found that, when induced by RANKL, curdlan suppressed osteoclast formation (Fig. 3, *A* and *B*), bone resorption (Fig. 3, *C* and *D*), and actin ring formation (Fig. 3*E*) in RAW 264.7 cells retrovirally transduced to overexpress dectin 1 (d-RAWs) as well as BMCs. On the basis of these findings, we speculate that dectin 1 is a principal receptor responsible for the regulation of osteoclast formation and activation mediated by curdlan. In contrast to d-RAWs, c-RAWs showed less responsiveness to the inhibitory effect of curdlan on RANKL-induced osteoclast formation. These findings are consistent with reports showing that RAW 264.7 cells express low levels of endogenous dectin 1, as measured by flow cytometry (10).

M-CSF and RANKL are essential and sufficient to promote osteoclastogenesis. M-CSF can induce the proliferation of BMCs and their differentiation into osteoclast precursors, and RANKL can subsequently induce the differentiation of osteoclast precursors into mature osteoclasts (29, 35). This study revealed that curdlan had no effect on M-CSF-induced BMC proliferation and differentiation, whereas curdlan inhibited RANKL-induced differentiation of osteoclast precursors into osteoclasts at early stages (Fig. 4). These data are also supported by the finding that curdlan had little effect on the expression of RANK protein induced by M-CSF (data not shown). We also demonstrated that curdlan had no effect on bone resorption activity and actin ring formation of mature osteoclasts (Fig. 5). Together, these results indicate that curdlan suppressed RANKL-induced osteoclastogenesis at the step of osteoclast precursor differentiation into mature osteoclasts and suggests that curdlan modulated the RANKL signaling pathway.

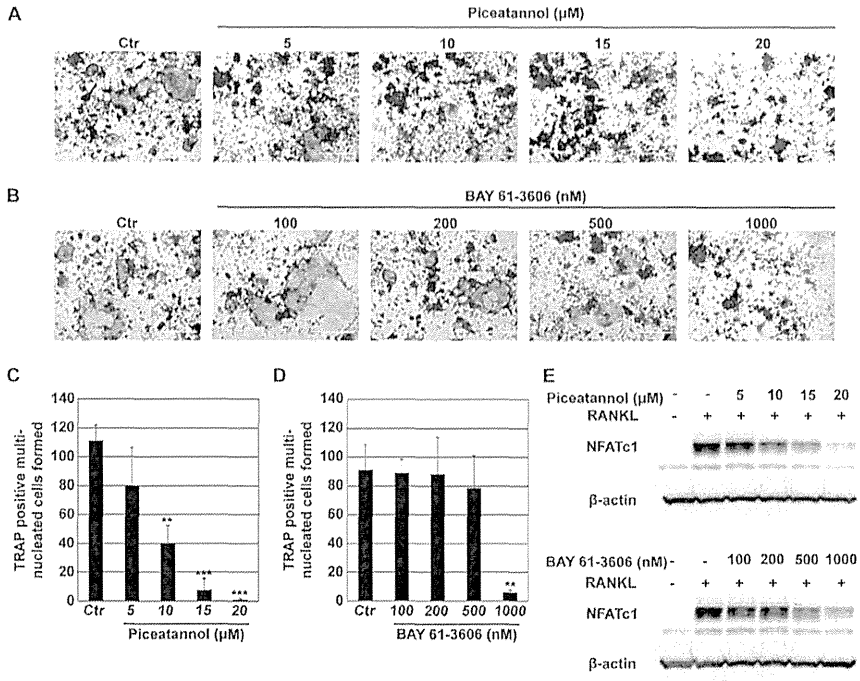

FIGURE 11. **Effect of selective inhibitor for Syk on RANKL-induced osteoclastogenesis in d-RAWs.** d-RAWs were pretreated with 5–20 μM of piceatannol (*A*) or 100–1000 nM of BAY 61-3606 (*B*) for 1 h. Cells were then incubated in the presence of RANKL (40 ng/ml) for 7 days. Cells were stained for TRAP activity. *Scale bars* = 500 μm. The number of osteoclasts differentiated from piceatannol-pretreated (*C*) and BAY 61-3606-pretreated (*D*) cells were counted after staining for TRAP activity. Data show the number of osteoclasts from three independent samples, and *error bars* represent mean ± S.D. Data were analyzed by Dunnett's test after one-way ANOVA. **, $p < 0.01$; ***, $p < 0.0001$ in comparison with the control without inhibitor pretreatment. *E*, d-RAWs were pretreated with piceatannol (5–20 μM) or BAY 61-3606 (100–1000 nM) for 1 h. Cells were then incubated in the presence or absence of RANKL (40 ng/ml) for 72 h. Whole cell lysates were subjected to SDS-PAGE and Western blot analyses, with the blots probed for NFATc1. Equivalent protein aliquots of cell lysates were also analyzed for β-actin.

Previous studies have demonstrated that NFATc1 is strongly induced by RANKL and is required for terminal differentiation of osteoclasts (30, 47). We found that the level of NFATc1 expression during osteoclastogenesis was decreased by curdlan in d-RAWs and BMCs. In contrast, we did not observe a change in RANKL-induced NFATc1 expression in c-RAWs treated with curdlan (Fig. 6). These results indicate that curdlan-dectin 1 interaction impairs RANKL-induced osteoclastogenesis via suppression of NFATc1.

The inhibitory effect of curdlan on osteoclastogenesis was also confirmed by evaluating RANKL-induced mRNA expression levels of osteoclast-related genes. TRAP (48), cathepsin K (49), and MMP9 (50) are required for the bone resorptive activity of mature osteoclast, whereas osteoclast stimulatory transmembrane protein is essential for cell-cell fusion of osteoclasts (51). On the basis of promoter analyses, TRAP (30, 52, 53), cathepsin K (52, 54), and MMP9 (55) are regulated by NFATc1. In addition, a study using a specific inhibitor of NFAT revealed that osteoclast stimulatory transmembrane protein expression also requires NFATc1 in osteoclasts (51). Our results show that curdlan markedly decreased osteoclast-related gene expression regulated by NFATc1 in d-RAWs (Fig. 7). It is possible that the curdlan-dectin 1 interaction changes the RANKL-NFATc1 axis, with an ultimate decrease in osteoclast development, in addition to decreased NFATc1 production.

We also examined the mechanism by which curdlan suppressed RANKL-mediated NFATc1 expression. NF-κB is involved in the activation of immediate-early responsive genes to RANKL (56) and is important for the initial induction of NFATc1 (57). On the other hand, NFATc1 is activated and binds its own promoter. After the induction of NFATc1, the combination of an AP-1 complex containing c-fos and the continuous activation of calcium signaling allows for the sustained autoamplification of NFATc1 (57). Western blot analysis revealed that curdlan inhibited RANKL-stimulated c-fos protein expression but not activation of NF-κB (Fig. 8). These findings led us to speculate that inhibition of RANKL-stimulated NFATc1 expression by curdlan in d-RAWs, may occur because of suppression of AP-1 signaling pathway, which regulates autoamplification of NFATc1. This speculation was strongly supported by the observation that curdlan interferes with RANKL-induced nuclear translocation of NFATc1 (Fig. 9). However, curdlan itself appears to increase phosphorylation of c-jun protein in d-RAWs but not c-RAWs, and activation of c-fos by RANKL was lower in d-RAWs than c-RAWs, indicating an alternative signaling pathway in osteoclastogenesis by curdlan. We have no precise explanation for this phenomenon, and further studies are required to identify the detailed regulatory mechanisms of dectin 1 on osteoclast formation. The molecular mechanisms of the interaction between curdlan and dectin 1 are currently under investigation using dectin 1-deficient mice.

Syk has been identified to be involved in dectin 1 signaling, which is activated by engagement with β-glucan (12, 21, 58). Interestingly, treatment with curdlan increased Syk protein degradation in d-RAWs (Fig. 10, *A* and *B*), suggesting that sup-

pression of dectin 1/Syk signaling by curdlan inhibits RANKL-induced osteoclastogenesis. However, real-time RT-PCR analysis revealed that curdlan treatment did not alter mRNA expression of Syk in d-RAWs (data not shown). On the other hand, the addition of curdlan significantly increased the level of phosphorylated Syk in d-RAWs. A previous study using B cells reported that, subsequent to ITAM binding, Syk was phosphorylated on tyrosine 323, which generated a binding site for ubiquitin ligase, resulting in Syk ubiquitination and down-regulation of downstream signaling (59). From these results, the molecular mechanism for posttranslational modifications, including phosphorylation, ubiquitination, SUMOylation, acetylation, and *O*-glycosylation, are currently under investigation in our laboratory.

The importance of the dectin 1-Syk interaction in osteoclastogenesis was demonstrated clearly by the dramatic decrease in osteoclast formation (Fig. 10, *E* and *F*) and NFATc1 expression (Fig. 10*G*) induced by Syk knockdown. These findings are consistent with a previous study that reported that osteoclasts from $Syk^{-/-}$ precursors (obtained from bone marrow chimeras generated using $Syk^{-/-}$ fetal liver cells) (60) failed to differentiate normally *in vitro* (24).

Syk is a tyrosine kinase and a key mediator of ITAM receptor signaling (61), which is an important regulatory mechanism in osteoclast differentiation and activity (25, 62). We also found chemical inhibitors of Syk, down-regulated osteoclast formation (Fig. 11, *A–D*), and NFATc1 expression (Fig. 11*E*) induced by RANKL. These results are consistent with the premise that curdlan is a potent negative regulator of Syk signaling in osteoclasts. Taken together, the findings obtained in this study suggest that curdlan-dectin 1 binding strongly inhibits NFATc1 expression during osteoclast formation through down-regulation of Syk signaling in osteoclast progenitor cells. Therefore, one might expect that the curdlan administration could be a potential candidate for the treatment of osteoclast-related diseases such as osteoporosis.

REFERENCES

1. Suda, T., Takahashi, N., and Martin, T. J. (1992) Modulation of osteoclast differentiation. *Endocr. Rev.* **13,** 66–80
2. Suda, T., Takahashi, N., Udagawa, N., Jimi, E., Gillespie, M. T., and Martin, T. J. (1999) Modulation of osteoclast differentiation and function by the new members of the tumor necrosis factor receptor and ligand families. *Endocr. Rev.* **20,** 345–357
3. Darnay, B. G., Haridas, V., Ni, J., Moore, P. A., and Aggarwal, B. B. (1998) Characterization of the intracellular domain of receptor activator of NF-κB (RANK): interaction with tumor necrosis factor receptor-associated factors and activation of NF-κB and c-Jun N-terminal kinase. *J. Biol. Chem.* **273,** 20551–20555
4. Asagiri, M., and Takayanagi, H. (2007) The molecular understanding of osteoclast differentiation. *Bone* **40,** 251–264
5. Janeway, C. A. Jr. (1989) Approaching the asymptote? Evolution and revolution in immunology. *Cold Spring Harbor Symp. Quant. Biol.* **54,** 1–13
6. Brown, G. D., Gordon, S. (2001) Immune recognition: a new receptor for β-glucans. *Nature* **413,** 36–37
7. Ariizumi, K., Shen, G. L., Shikano, S., Xu, S., Ritter, R., 3rd, Kumamoto, T., Edelbaum, D., Morita, A., Bergstresser, P. R., and Takashima, A. (2000) Identification of a novel, dendritic cell-associated molecule, dectin-1, by subtractive cDNA cloning. *J. Biol. Chem.* **275,** 20157–20167
8. Taylor, P. R., Brown, G. D., Reid, D. M., Willment, J. A., Martinez-Pomares, L., Gordon, S., and Wong, S. Y. (2002) The β-glucan receptor, dectin-1, is predominantly expressed on the surface of cells of the monocyte/macrophage and neutrophil lineages. *J. Immunol.* **169,** 3876–3882
9. Brown, G. D., Taylor, P. R., Reid, D. M., Willment, J. A., Williams, D. L., Martinez-Pomares, L., Wong, S. Y., and Gordon, S. (2002) Dectin-1 is a major β-glucan receptor on macrophages. *J. Exp. Med.* **196,** 407–412
10. Brown, G. D., Herre, J., Williams, D. L., Willment, J. A., Marshall, A. S., and Gordon, S. (2003) Dectin-1 mediates the biological effects of β-glucans. *J. Exp. Med.* **197,** 1119–1124
11. Rogers, N. C., Slack, E. C., Edwards, A. D., Nolte, M. A., Schulz, O., Schweighoffer, E., Williams, D. L., Gordon, S., Tybulewicz, V. L., Brown, G. D., and Reis e Sousa, C. (2005) Syk-dependent cytokine induction by Dectin-1 reveals a novel pattern recognition pathway for C type lectins. *Immunity* **22,** 507–517
12. Underhill, D. M., Rossnagle, E., Lowell, C. A., and Simmons, R. M. (2005) Dectin-1 activates Syk tyrosine kinase in a dynamic subset of macrophages for reactive oxygen production. *Blood* **106,** 2543–2550
13. Drummond, R. A., Saijo, S., Iwakura, Y., and Brown, G. D. (2011) The role of Syk/CARD9 coupled C-type lectins in antifungal immunity. *Eur. J. Immunol.* **41,** 276–281
14. Osorio, F., and Reis e Sousa C. (2011) Myeloid C-type lectin receptors in pathogen recognition and host defense. *Immunity* **34,** 651–664
15. Brown, G. D., and Gordon, S. (2003) Fungal β-glucans and mammalian immunity. *Immunity* **19,** 311–315
16. Czop, J. K. (1986) The role of β-glucan receptors on blood and tissue leukocytes in phagocytosis and metabolic activation. *Pathol. Immunopathol. Res.* **5,** 286–296
17. Williams, D. L. (1997) Overview of (1→3)-β-D-glucan immunobiology. *Mediators Inflamm.* **6,** 247–250
18. Ross, G. D., Vetvicka, V., Yan, J., Xia, Y., and Vetvicková, J. (1999) Therapeutic intervention with complement and β-glucan in cancer. *Immunopharmacology* **42,** 61–74
19. Williams, D. L., Mueller, A., and Browder, W. (1996) Glucan-based macrophage stimulators. *Clin. Immunotherapeutics* **5,** 392–399
20. Castro, G. R., Panilaitis, B., Bora, E., and Kaplan, D. L. (2007) Controlled release biopolymers for enhancing the immune response. *Mol. Pharm.* **4,** 33–46
21. Mocanu, G., Mihai, D., Moscovici, M., Picton, L., LeCerf, D. (2009) Curdlan microspheres: synthesis, characterization and interaction with proteins (enzymes, vaccines). *Int. J. Biol. Macromol.* **44,** 215–221
22. Koga, T., Inui, M., Inoue, K., Kim, S., Suematsu, A., Kobayashi, E., Iwata, T., Ohnishi, H., Matozaki, T., Kodama, T., Taniguchi, T., Takayanagi, H., and Takai, T. (2004) Costimulatory signals mediated by the ITAM motif cooperate with RANKL for bone homeostasis. *Nature* **428,** 758–763
23. Faccio, R., Zou, W., Colaianni, G., Teitelbaum, S. L., and Ross, F. P. (2003) High dose M-CSF partially rescues the $Dap12^{-/-}$ osteoclast phenotype. *J. Cell Biochem.* **90,** 871–883
24. Mócsai, A., Humphrey, M. B., Van Ziffle, J. A., Hu, Y., Burghardt, A., Spusta, S. C., Majumdar, S., Lanier, L. L., Lowell, C. A., and Nakamura, M. C. (2004) The immunomodulatory adapter proteins DAP12 and Fc receptor γ-chain (FcRγ) regulate development of functional osteoclasts through the Syk tyrosine kinase. *Proc. Natl. Acad. Sci. U.S.A.* **101,** 6158–6163
25. Zou, W., Kitaura, H., Reeve, J., Long, F., Tybulewicz, V. L., Shattil, S. J., Ginsberg, M. H., Ross, F. P., and Teitelbaum, S. L. (2007) Syk, c-Src, the αvβ3 integrin, and ITAM immunoreceptors, in concert, regulate osteoclastic bone resorption. *J. Cell Biol.* **176,** 877–888
26. Saltel, F., Destaing, O., Bard, F., Eichert, D., and Jurdic, P. (2004) Apatite-mediated actin dynamics in resorbing osteoclasts. *Mol. Biol. Cell* **15,** 5231–5241
27. Boyce, B. F., Yoneda, T., Lowe, C., Soriano, P., and Mundy, G. R. (1992) Requirement of pp60c-src expression for osteoclasts to form ruffled borders and resorb bone in mice. *J. Clin. Invest.* **90,** 1622–1627
28. Teitelbaum, S. L., and Ross, F. P. (2003) Genetic regulation of osteoclast development and function. *Nat. Rev. Genet.* **4,** 638–649
29. Takahashi, N., Udagawa, N., Tanaka, S., and Suda, T. (2003) Generating murine osteoclasts from bone marrow. *Methods Mol. Med.* **80,** 129–144
30. Takayanagi, H., Kim, S., Koga, T., Nishina, H., Isshiki, M., Yoshida, H., Saiura, A., Isobe, M., Yokochi, T., Inoue, J., Wagner, E. F., Mak, T. W., Kodama, T., and Taniguchi, T. (2002) Induction and activation of the

transcription factor NFATc1 (NFAT2) integrate RANKL signaling in terminal differentiation of osteoclasts. *Dev. Cell.* **3,** 889–901
31. Eiseman, E., and Bolen, J. B. (1992) Engagement of the high-affinity IgE receptor activates Src protein-related tyrosine kinases. *Nature* **355,** 78–80
32. Yamamoto, N., Takeshita, K., Shichijo, M., Kokubo, T., Sato, M., Nakashima, K., Ishimori, M., Nagai, H., Li, Y. F., Yura, T., and Bacon, K. B. (2003) The orally available spleen tyrosine kinase inhibitor 2-[7-(3,4-dimethoxyphenyl)-imidazo[1,2-*c*]pyrimidin-5-ylamino] nicotinamide dihydrochloride (BAY 61-3606) blocks antigen-induced airway inflammation in rodents. *J. Pharmacol. Exp. Ther.* **306,** 1174–1181
33. Adachi, Y., Ishii, T., Ikeda, Y., Hoshino, A., Tamura, H., Aketagawa, J., Tanaka, S., and Ohno, N. (2004) Characterization of β-glucan recognition site on C-type lectin, dectin-1. *Infect. Immun.* **72,** 4159–4171
34. Chaung, H. C., Huang, T. C., Yu, J. H., Wu, M. L., Chung, W. B. (2009) Immunomodulatory effects of β-glucans on porcine alveolar macrophages and bone marrow haematopoietic cell-derived dendritic cells. *Vet. Immunol. Immunopathol.* **131,** 147–157
35. Takayanagi, H. (2007) Osteoimmunology: shared mechanisms and crosstalk between the immune and bone systems. *Nat. Rev. Immunol.* **7,** 292–304
36. Brown, G. D. (2006) Dectin-1: a signalling non-TLR pattern-recognition receptor. *Nat. Rev. Immunol.* **6,** 33–43
37. Willment, J. A., Gordon, S., and Brown, G. D. (2001) Characterization of the human β-glucan receptor and its alternatively spliced isoforms. *J. Biol. Chem.* **276,** 43818–43823
38. Kerrigan, A. M., Brown, G. D. (2009) C-type lectins and phagocytosis. *Immunobiology* **214,** 562–575
39. Kataoka, K., Muta, T., Yamazaki, S., and Takeshige, K. (2002) Activation of macrophages by linear (1right-arrow3)-β-D-glucans: implications for the recognition of fungi by innate immunity. *J. Biol. Chem.* **277,** 36825–36831
40. Gantner, B. N., Simmons, R. M., Canavera, S. J., Akira, S., and Underhill, D. M. (2003) Collaborative induction of inflammatory responses by dectin-1 and Toll-like receptor 2. *J. Exp. Med.* **197,** 1107–1117
41. Palma, A. S., Feizi, T., Zhang, Y., Stoll, M. S., Lawson, A. M., Díaz-Rodríguez, E., Campanero-Rhodes, M. A., Costa, J., Gordon, S., Brown, G. D., and Chai, W. (2006) Ligands for the β-glucan receptor, Dectin-1, assigned using "designer" microarrays of oligosaccharide probes (neoglycolipids) generated from glucan polysaccharides. *J. Biol. Chem.* **281,** 5771–5779
42. UCAS Japan Investigators, Morita, A., Kirino, T., Hashi, K., Aoki, N., Fukuhara, S., Hashimoto, N., Nakayama, T., Sakai, M., Teramoto, A., Tominari, S., and Yoshimoto, T. (2012) The natural course of unruptured cerebral aneurysms in a Japanese cohort. *N. Engl. J. Med.* **366,** 2474–2482
43. Fuller, K., Thong, J. T., Breton, B. C., and Chambers, T. J. (1994) Automated three-dimensional characterization of osteoclastic resorption lacunae by stereoscopic scanning electron microscopy. *J. Bone Miner. Res.* **9,** 17–23
44. Teti, A., Marchisio, P. C., and Zallone, A. Z. (1991) Clear zone in osteoclast function: role of podosomes in regulation of bone-resorbing activity. *Am. J. Physiol.* **261,** C1-C7
45. Zou, W., and Teitelbaum, S. L. (2010) Integrins, growth factors, and the osteoclast cytoskeleton. *Ann. N.Y. Acad. Sci.* **1192,** 27–31
46. Hsu, H., Lacey, D. L., Dunstan, C. R., Solovyev, I., Colombero, A., Timms, E., Tan, H. L., Elliott, G., Kelley, M. J., Sarosi, I., Wang, L., Xia, X. Z., Elliott, R., Chiu, L., Black, T., Scully, S., Capparelli, C., Morony, S., Shimamoto, G., Bass, M. B., and Boyle, W. J. (1999) Tumor necrosis factor receptor family member RANK mediates osteoclast differentiation and activation induced by osteoprotegerin ligand. *Proc. Natl. Acad. Sci. U.S.A.* **96,** 3540–3545
47. Ishida, N., Hayashi, K., Hoshijima, M., Ogawa, T., Koga, S., Miyatake, Y., Kumegawa, M., Kimura, T., and Takeya, T. (2002) Large scale gene expression analysis of osteoclastogenesis *in vitro* and elucidation of NFAT2 as a key regulator. *J. Biol. Chem.* **277,** 41147–41156
48. Halleen, J. M., Räisänen, S., Salo, J. J., Reddy, S. V., Roodman, G. D., Hentunen, T. A., Lehenkari, P. P., Kaija, H., Vihko, P., and Väänänen, H. K. (1999) Intracellular fragmentation of bone resorption products by reactive oxygen species generated by osteoclastic tartrate-resistant acid phosphatase. *J. Biol. Chem.* **274,** 22907–22910
49. Ishikawa, T., Kamiyama, M., Tani-Ishii, N., Suzuki, H., Ichikawa, Y., Hamaguchi, Y., Momiyama, N., and Shimada, H. (2001) Inhibition of osteoclast differentiation and bone resorption by cathepsin K antisense oligonucleotides. *Mol. Carcinog.* **32,** 84–91
50. Ishibashi, O., Niwa, S., Kadoyama, K., and Inui, T. (2006) MMP-9 antisense oligodeoxynucleotide exerts an inhibitory effect on osteoclastic bone resorption by suppressing cell migration. *Life Sci.* **79,** 1657–1660
51. Miyamoto, H., Suzuki, T., Miyauchi, Y., Iwasaki, R., Kobayashi, T., Sato, Y., Miyamoto, K., Hoshi, H., Hashimoto, K., Yoshida, S., Hao, W., Mori, T., Kanagawa, H., Katsuyama, E., Fujie, A., Morioka, H., Matsumoto, M., Chiba, K., Takeya, M., Toyama, Y., and Miyamoto, T. (2012) Osteoclast stimulatory transmembrane protein and dendritic cell-specific transmembrane protein cooperatively modulate cell-cell fusion to form osteoclasts and foreign body giant cells. *J. Bone Miner. Res.* **27,** 1289–1297
52. Kim, Y., Sato, K., Asagiri, M., Morita, I., Soma, K., and Takayanagi, H. (2005) Contribution of nuclear factor of activated T cells c1 to the transcriptional control of immunoreceptor osteoclast-associated receptor but not triggering receptor expressed by myeloid cells-2 during osteoclastogenesis. *J. Biol. Chem.* **280,** 32905–32913
53. Matsuo, K., Galson, D. L., Zhao, C., Peng, L., Laplace, C., Wang, K. Z., Bachler, M. A., Amano, H., Aburatani, H., Ishikawa, H., and Wagner, E. F. (2004) Nuclear factor of activated T-cells (NFAT) rescues osteoclastogenesis in precursors lacking c-Fos. *J. Biol. Chem.* **279,** 26475–26480
54. Matsumoto, M., Kogawa, M., Wada, S., Takayanagi, H., Tsujimoto, M., Katayama, S., Hisatake, K., Nogi, Y. (2004) Essential role of p38 mitogen-activated protein kinase in cathepsin K gene expression during osteoclastogenesis through association of NFATc1 and PU. 1. *J. Biol. Chem.* **279,** 45969–45979
55. Song, I., Kim, J. H., Kim, K., Jin, H. M., Youn, B. U., Kim, N. (2009) Regulatory mechanism of NFATc1 in RANKL-induced osteoclast activation. *FEBS Lett.* **583,** 2435–2440
56. Takatsuna, H., Asagiri, M., Kubota, T., Oka, K., Osada, T., Sugiyama, C., Saito, H., Aoki, K., Ohya, K., Takayanagi, H., and Umezawa K. (2005) Inhibition of RANKL-induced osteoclastogenesis by (-)-DHMEQ, a novel NF-κB inhibitor, through downregulation of NFATc1. *J. Bone Miner. Res.* **20,** 653–662
57. Asagiri, M., Sato, K., Usami, T., Ochi, S., Nishina, H., Yoshida, H., Morita, I., Wagner, E. F., Mak, T. W., Serfling, E., and Takayanagi, H. (2005) Autoamplification of NFATc1 expression determines its essential role in bone homeostasis. *J. Exp. Med.* **202,** 1261–1269
58. Gross, O., Gewies, A., Finger, K., Schäfer, M., Sparwasser, T., Peschel, C., Förster, I., and Ruland, J. (2006) Card9 controls a non-TLR signalling pathway for innate anti-fungal immunity. *Nature* **442,** 651–656
59. Rao, N., Dodge, I., and Band, H. (2002) The Cbl family of ubiquitin ligases: critical negative regulators of tyrosine kinase signaling in the immune system. *J. Leukocyte Biol.* **71,** 753–763
60. Mócsai, A., Zhou, M., Meng, F., Tybulewicz, V. L., and Lowell, C. A. (2002) Syk is required for integrin signaling in neutrophils. *Immunity* **16,** 547–558
61. Humphrey, M. B., Lanier, L. L., and Nakamura, M. C. (2005) Role of ITAM-containing adapter proteins and their receptors in the immune system and bone. *Immunol. Rev.* **208,** 50–65
62. Solski, P. A., Wilder, R. S., Rossman, K. L., Sondek, J., Cox, A. D., Campbell, S. L., and Der, C. J. (2004) Requirement for C-terminal sequences in regulation of Ect2 guanine nucleotide exchange specificity and transformation. *J. Biol. Chem.* **279,** 25226–25233

ARCHIVES OF ORAL BIOLOGY 59 (2014) 835–840

Available online at www.sciencedirect.com

ScienceDirect

journal homepage: http://www.elsevier.com/locate/aob

Inhibitory effects of ameloblastin on epithelial cell proliferation

Noriko Saito [a,b], *Wataru Ariyoshi* [a,*], *Toshinori Okinaga* [a], *Mariko Kamegawa* [c], *Miho Matsukizono* [c], *Yasuo Akebiyama* [c], *Chiaki Kitamura* [b], *Tatsuji Nishihara* [a]

[a] *Division of Infections and Molecular Biology, Department of Health Promotion, Kyushu Dental University, 2-6-1 Manazuru, Kokurakita-ku, Kitakyushu, Fukuoka 803-8580, Japan*

[b] *Division of Pulp Biology, Operative Dentistry and Endodontics, Department of Cariology and Periodontology, Kyushu Dental University, 2-6-1 Manazuru, Kokurakita-ku, Kitakyushu, Fukuoka 803-8580, Japan*

[c] *Genenet Co., Ltd, 5-22-8, Tanotsu, Higashi-Ku, Fukuoka 813-0034, Japan*

ARTICLE INFO

Article history:
Accepted 5 May 2014

Keywords:
Ameloblastin
Protein purification
Periodontitis
Epithelial cell proliferation
Cell cycle
Apoptosis

ABSTRACT

Objective: Ameloblastin is an enamel matrix protein expressed in several tissues. Many potential mechanisms have been identified by which ameloblastin functions as an extracellular matrix protein. However, the biological effects of ameloblastin on gingival epithelial cells remain unclear. In the present study, we established a novel system to purify recombinant human ameloblastin and clarified its biological functions in epithelial cells *in vitro*.

Design: Recombinant human ameloblastin was isolated from COS-7 cells overexpressing HaloTag®-fused human ameloblastin by the HaloTag® system and then purified further by reverse-phase high-performance liquid chromatography. SCC-25 cells, derived from human oral squamous cell carcinoma, were treated with recombinant ameloblastin and then cell survival was assessed by a WST-1 assay. Cell cycle analysis was performed by flow cytometry.

Results: The novel purification system allowed effective recovery of the recombinant ameloblastin proteins at a high purity. Recombinant ameloblastin protein was found to suppress the proliferation of SCC-25 cells. Flow cytometric analysis showed that ameloblastin treatment induced cell cycle arrest G1 phase.

Conclusions: We developed a procedure for production of highly purified recombinant human ameloblastin. Biological analyses suggest that ameloblastin induces cell cycle arrest in epithelial cells and regulates the progression of periodontitis.

1. Introduction

Periodontitis is one of the most common chronic inflammatory diseases characterized by the destruction of tooth-supporting structures.[1] It is a complex disease resulting from the combination of the direct effects of microbial virulence factors and the host response to microbial challenge.[2,3] Although numerous microbial aetiologies have been reported for periodontitis, its pathogenesis remains to be elucidated because of the complexity of host–microbial interactions.

* *Corresponding author.* Tel.: +81 93 285 3052; fax: +81 93 581 4984.
E-mail address: arikichi@kyu-dent.ac.jp (W. Ariyoshi).

http://dx.doi.org/10.1016/j.archoralbio.2014.05.010
0003–9969/

The gingiva is covered by a stratified squamous epithelium that constantly receives local stimuli. The gingival epithelium can serve as the first line of defense against bacterial invasion.[4] In addition to its function as a physical and chemical barrier, the gingival epithelium plays a crucial role in the immune response against infectious inflammation in periodontal tissue by expression of a large variety of cytokines and antimicrobial peptides.[5–8] Therefore, the gingival epithelium plays a critical role in maintaining mucosal homeostasis, and the loss of the epithelial barrier function is thought to contribute towards periodontitis progression.

Ameloblastin, a matrix adhesion protein also known as sheathlin and amelin, was first detected in secretory stage ameloblasts.[9,10] It is also expressed by osteoblasts,[11] cementoblasts,[12] and epithelial rests of Malassez in the periodontal ligament.[13] Ameloblastin contains a fibronectin interaction sites,[14] several heparin-binding domains,[15,16] a potential $\alpha 2\beta 1$ integrin-binding domain, and a thrombospondin cell adhesion motif,[17] which might be responsible for the interaction of ameloblastin with the surface of dental epithelial cells.

Ameloblastin was initially reported to involved in the regulation of ameloblasts.[18] Many potential mechanisms have been identified by which ameloblastin functions as an extracellular matrix protein, including the regulation of enamel biomineralisation[19–21] and osteoblast differentiation.[22] Furthermore, recent studies have suggested that ameloblastin may act as a signalling molecule[23,24] and possesses growth factor activity.[25]

In our previous study, we purified bioactive fractions from enamel matrix derivative (EMD) and revealed that ameloblastin is a candidate component that inhibits epithelial cell proliferation (unpublished data). However, the detailed mechanism by which ameloblastin inhibits epithelial cell proliferation has not because of the difficulty of discriminating the responses induced by ameloblastin from those caused by other proteins that often contaminate ameloblastin preparations. In the present study, we purified recombinant ameloblastin protein using a novel fusion tag system and clarified its biological functions in epithelial cells *in vitro*.

2. Materials and methods

2.1. *Cell culture*

SCC-25 cells, derived from human squamous cell carcinoma of the tongue, were obtained from DS Pharmaceutical (Osaka, Japan) and maintained in a 1:1 mix of Dulbecco's modified Eagle's medium and Ham's F-12 (Nacalai Tesque, Kyoto, Japan) supplemented with 10% foetal bovine serum (Gibco, Grand Island, NY, USA), penicillin G (100 U/ml) and streptomycin (100 μg/ml).

2.2. *Expression and purification of recombinant ameloblastin*

The expression vector pFNA21A (FHC21950M; Promega KK, Tokyo, Japan) was used to express HaloTag®-fused human ameloblastin protein. Expression plasmids were transfected into COS-7 cells by electroporation using a NEPA21 Super Electroporator (Nepa Gene, Chiba, Japan). After 24 h, the transfected cells were lysed using a lysis buffer (50 mM Tris–HCl, 150 mM NaCl, 1% Triton X-100, and 0.1% sodium deoxycholate, pH 7.5). HaloTag® fusion recombinant protein was then partially purified by the HaloTag® Mammalian Protein Purification System (Promega KK) according to the manufacturer's instructions. The isolated fraction was lyophilised and then the recombinant ameloblastin was further purified by reverse-phase high-performance liquid chromatography (HPLC) using a Waters system (Medford, MA, USA) and C_{18} column (4.6 × 150 mm; Vydac, Hesperia, CA, USA) equilibrated with 0.1% trifluoroacetic acid. The fraction with one major peak was collected, diluted in culture medium, sterilised using a surfactant cellulose acetate membrane filter (0.20 μm pore size; Corning, NY, USA), and then used as purified recombinant ameloblastin in bioassays. Protein concentrations were measured using a DC™ protein assay (Bio-Rad Laboratories, Hercules, CA, USA).

2.3. *Preparation of a monoclonal antibody (mAb) against human ameloblastin*

Animal immunisation was performed by a standard procedure using recombinant ameloblastin as the immunogen. Ameloblastin (1.0 ml, 15 μg) was emulsified in an equal volume of Freund"s complete adjuvant (Difco Laboratories, Detroit, MI, USA) and then injected intraperitoneally into 7-week-old female Balb/c mice (Charles River Laboratories Japan, Yokohama, Japan). Then, at about 2-week intervals, Balb/c mice were administered with a booster injection of ameloblastin prepared in the same manner. After the second immunisation, the titre of antiserum was tested by an enzyme linked immunosorbent assay (ELISA).

Recombinant ameloblastin was diluted in coating buffer (50 mM $NaHCO_3$) to 1 μg/ml, added to the micro-titre plates (50 μl/well) as the coating antigen, and then incubated overnight at 4 °C. Plates coated with recombinant ameloblastin were washed three times with PBST (PBS containing 0.05% Tween-20) and then blocked with 1% Block Ace (DS Pharma Biomedical, Osaka, Japan) at room temperature for 2 h. After three washes with PBST, serial dilutions of antiserum (50 μl/well) were added to the plates, followed by incubation at room temperature for 2 h. After washing, horseradish peroxidase (HRP)-conjugated goat anti-mouse IgG (Santa Cruz Biotechnology, Santa Cruz, CA, USA) in PBST was added to the reaction wells, followed by incubation at room temperature for 30 min. After five washes with PBST, SigmaFast OPD tablet set (Sigma–Aldrich, St. Louis, MO, USA) was added to the wells for colour development, and then 10% H_2SO_4 was added to stop the reaction. The absorbance was measured at 490 nm by a microplate reader (Thermo Fisher Scientific, Waltham, MA, USA).

The immunised mouse with a high serum titre was given an intravenous injection with of 5 μg ameloblastin. After 4 days, the B cells were isolated from spleen and fused with P3U1 myeloma cells at a ratio of 1:5 by polyethylene glycol 1500. Then, the cells were cultured in 96-well plates containing HAT medium at 37 °C with 5% CO_2. After about 10 days, the HAT medium was changed to HT medium. After 2 days, the culture supernatants were tested by ELISA and positive clones

were obtained by limiting dilutions until the positive percentage reached 100%. Preparation of the mAb from hybridoma supernatants was carried out using a HiTRAP Protein G HP affinity column (GE Healthcare UK, Amersham, Buckinghamshire, UK). The reactivity and specificity of the purified mAb were analysed by Western blotting.

2.4. Western blotting

Purified ameloblastin protein was subjected to SDS-polyacrylamide gel electrophoresis (PAGE) and the separated proteins were transferred to a polyvinylidene fluoride membrane (Immobilon P; Millipore, Billerica, MA, USA). Nonspecific binding sites were blocked by incubating the membrane in Blocking One (Nacalai Tesque) at room temperature for 60 min. The membrane was then incubated with an anti-ameloblastin polyclonal antibody (Santa Cruz Biotechnology) or the anti-ameloblastin mAb at 4 °C overnight. Immune complexes were detected by incubation with an HRP-conjugated secondary antibody (Molecular Probes, Carlsbad, CA, USA) at room temperature for 1 h. After washing the membranes, chemiluminescence was produced using ECL reagent (Amersham Pharmacia Biotech, Uppsala, Sweden) and detected digitally with the GelDoc™ XR Plus System (Bio-Rad Laboratories).

2.5. WST-1 analysis

Cell viability was determined using tetrazolium salt WST-1 (4-[3-(4-iodophenyl)-2H-5-tetrazolio]-1-3-benzene disulfonate; Dojindo Laboratories, Kumamoto, Japan). SCC-25 cells (1×10^4 cells/well) were seeded in 96-well plates and cultured for 6 h. The cells were then stimulated with recombinant ameloblastin for 48 h. WST-1 solution (10 μl) was then added to each well, followed by incubation for 2 h. Absorbances at 450 and 630 nm were measured using a Multiskan JX Microplate Reader (Thermo Electron, Kanagawa, Japan).

2.6. Flow cytometric analysis

To analyse the cell cycle, SCC-25 cells (1.5×10^5 cells/ml) were suspended in a hypotonic solution (0.1% sodium citrate, 0.2% NP-40, and 0.25 mg/ml RNase, pH 8.0) and then stained with 50 μg/ml propidium iodide (PI). DNA content was then analysed using an EPICS XL (Beckman Coulter, Fullerton, CA, USA). The percentage of cells in each cell cycle phase was determined by MultiCycle for Windows (Phoenix Flow Systems, San Diego, CA, USA).

2.7. Statistics analysis

Data are expressed as mean values ± standard deviation (SD) of three experiments. Statistical analysis was performed by one-way analysis of variance (ANOVA), followed by Dunnett's test. A value of $P < 0.05$ was considered significant. All statistical analyses were carried out using JMP® software version 10.0.2 (SAS Institute, Cary, NC, USA).

3. Results

3.1. Purification of recombinant human ameloblastin

Halo-ameloblastin and cleaved ameloblastin were purified using the HaloTag® Mammalian Protein Purification System (Fig. 1). First, the Halo-ameloblastin fusion protein was

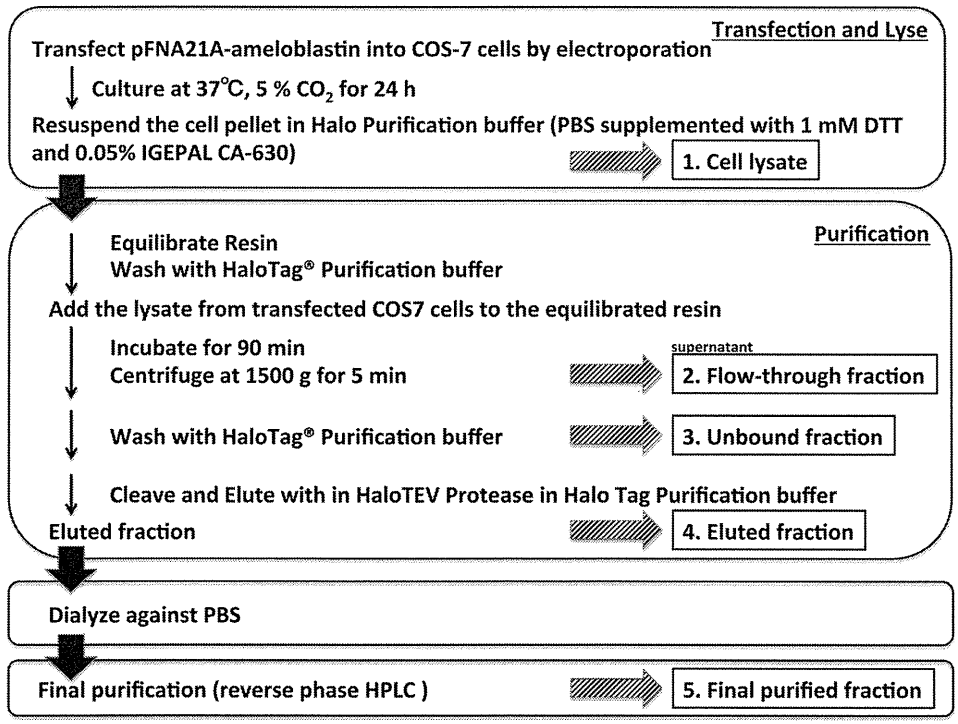

Fig. 1 – Purification of recombinant ameloblastin protein. Scheme of the protocol for recombinant ameloblastin purification.

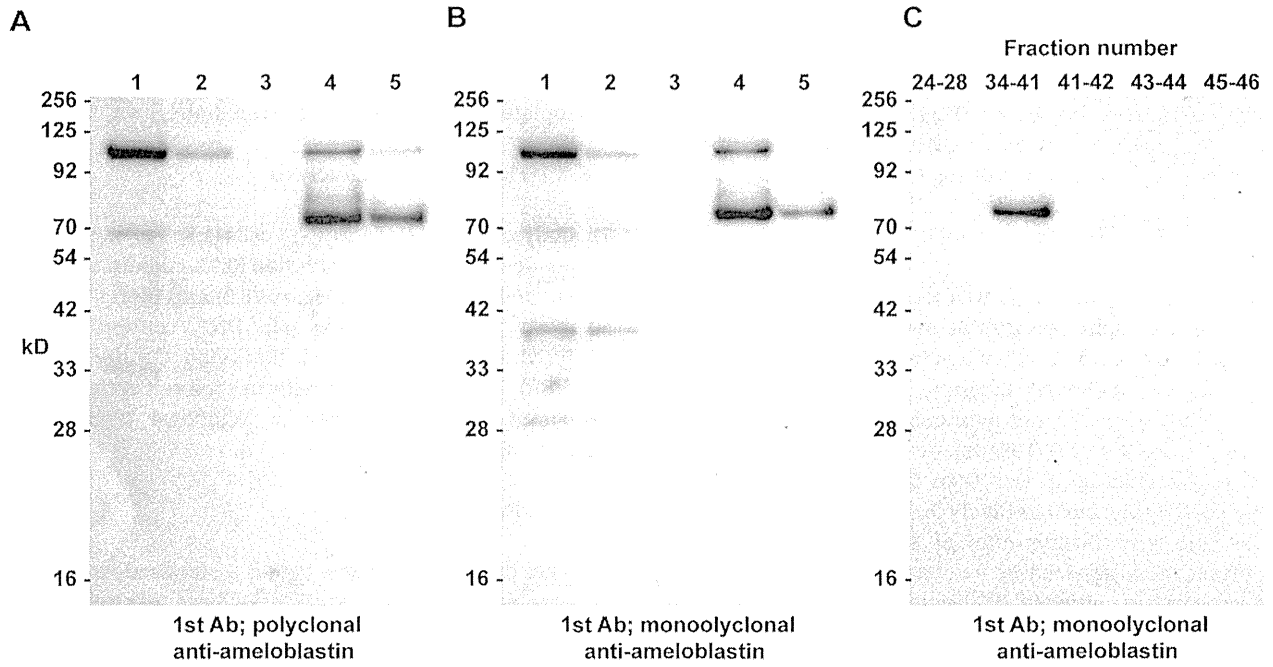

Fig. 2 – Detection of recombinant ameloblastin protein. Purified ameloblastin was subjected to 12.5% SDS-PAGE and western blot analyses. Blotted membranes were treated with a polyclonal antibody (A) and mAb (B) against ameloblastin. Lanes: (1) Total cell lysate transfected with the expression vector for HaloTag®-fused human ameloblastin proteins; (2) Flow-through after the sample was loaded onto HaloLink™ Resin; (3) HaloTag® Protein Purification Buffer wash; 4, Sample taken after inducing cleavage with TEV protease; 5, Final protein purified by reverse-phase HPLC. (C) Each fraction purified from reverse-phase HPLC was also subjected to 12.5% SDS-PAGE and western blot analysis using the anti-ameloblastin mAb.

subjected to HaloLink™ Resin. This step removed most of the other proteins. Purified Halo-ameloblastin was then digested by HaloTEV Protease. After dialysis, the cleaved ameloblastin protein was separated from residual uncleaved Halo-ameloblastin by reverse-phase HPLC.

Western blot analysis of recombinant ameloblastin showed a 105 kDa Halo-ameloblastin fusion protein before cleavage (Fig. 2A and B, lane 1). After cleavage, we detected a predominant immunoreactive band of 70 kDa (Fig. 2A and B, lane 5). As shown in Fig. 2C, ameloblastin was only observed in the fraction with a high peak in reverse-phase HPLC purification, whereas other fractions showed no immunoreactive band.

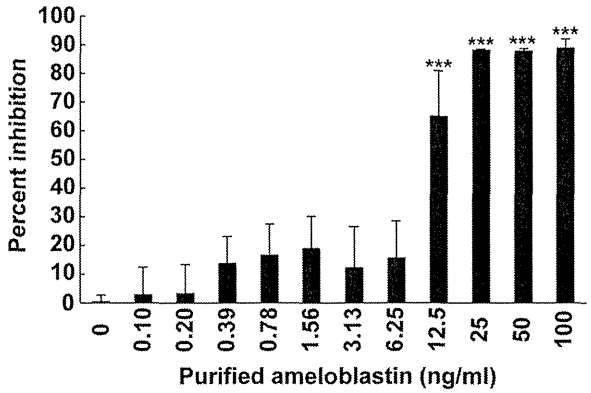

Fig. 3 – Effect of recombinant ameloblastin on epithelial cell proliferation. SCC-25 cells were stimulated with recombinant ameloblastin for 48 h, and then cell viability was determined by WST-1 analysis. Data show the percentage inhibition of cell proliferation from three independent samples. Bars represent the means + SD. Data were analysed by Dunnett's test after one-way ANOVA (*P < 0.0001 compared with the vehicle alone).**

3.2. *Effects of purified recombinant ameloblastin on epithelial cell proliferation*

To determine the effects of ameloblastin on cell viability, SCC-25 cells were treated with purified ameloblastin for 48 h, and then cell survival was assessed by a WST-1 assay. The proliferation of SCC-25 cells was inhibited when cultured with recombinant ameloblastin (Fig. 3). The effect of ameloblastin on cell proliferation was concentration-dependent and reached a maximum at 25 ng/ml (88% inhibition). Cells treated with the vehicle (1× PBS, pH 7.5, containing 1 mM dithiothreitol and 0.005% IGEPAL® CA630) showed no effects on cell viability (data not shown).

3.3. *Cell cycle arrest in epithelial cells induced by ameloblastin*

The effect of ameloblastin on the cell cycle of SCC-25 cells was examined by flow cytometric analysis. No change in the percentage of control cells treated with the vehicle in each phase was observed during the culture period (Fig. 4A). In contrast, the percentage of ameloblastin-treated cells in the G1 phase increased from 55.2 to 69.3% over 48 h of culture (Fig. 4B).

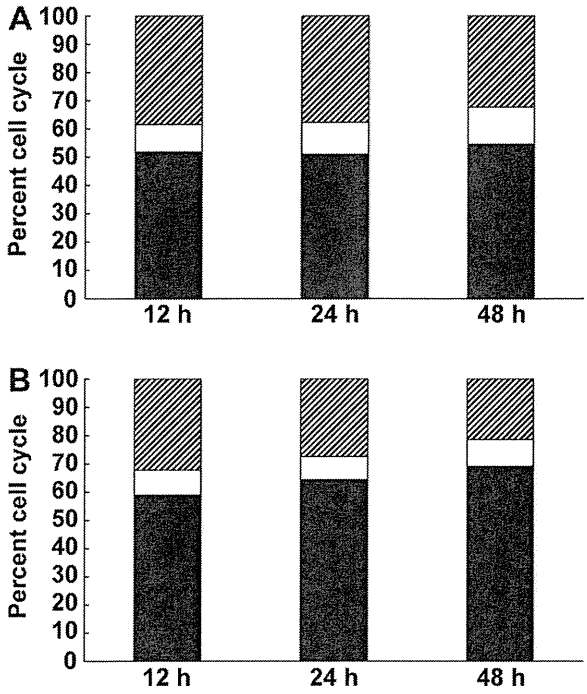

Fig. 4 – Effect of ameloblastin on the cell cycle in epithelial cells. SCC-25 cells were treated with ameloblastin (100 ng/ml) for the indicated times, and then stained with PI to determine the distribution during each phase of the cell cycle. (A) Vehicle-treated control cells. (B) Ameloblastin-treated cells. Data shown are representative of three independent experiments with similar results obtained in each. Solid bars percentage of cells in G1 phase; open bars percentage of cells in S phase; striped bars percentage in G2/M phase.

4. Discussion

Although cultured mammalian cells are preferred to produce functional mammalian proteins with appropriate post-translational modifications, purification of recombinant proteins is frequently hampered by low expression. The development of fusion tag systems is essential for purification and analysis of recombinant proteins.[26] The advantages of using fusion proteins to facilitate purification and detection of recombinant proteins are well recognised because of their reversible binding interactions with specific ligands. HaloTag® is a 34 kDa monomeric protein derived from a bacterial haloalkane dehalogenase, which was designed to covalently bind to a series of chloroalkane ligands.[27] Covalent bond formation between the protein tag and the chloroalkane linker is highly specific and occurs rapidly under physiological conditions.[28] Furthermore, cleavage of the HaloTag® does not result in protein insolubility. In the present study, we purified recombinant human ameloblastin from COS-7 cells over-expressing HaloTag®-fused human ameloblastin using the HaloTag® Mammalian Protein Purification System, followed by further purification using reverse-phase HPLC (Fig. 1). As shown in Fig. 1B and C, our purification system was found to be effective to purity and recover the recombinant ameloblastin proteins.

Western blotting analysis revealed that this novel method allowed highly efficient purification of recombinant ameloblastin (Fig. 2A). We also generated a highly specific mAb against human ameloblastin. In general, mAbs are used in scientific studies because of their specific and high affinity interactions with antigens. As shown in Fig. 2B and C, the anti-ameloblastin mAb exhibited high sensitivity and specificity for recombinant ameloblastin. These findings suggest that the mAb established in this study may facilitate further studies of the structure and function of ameloblastin and permit large-scale production of biologically active recombinant ameloblastin that is suitable for *in vivo* experiments.

Amelogenin and ameloblastin have been reported to exhibit growth factor-like activities in periodontal ligament cells.[25] However, less attention has been paid to the effects of ameloblastin on epithelial cell proliferation. In the present study, recombinant ameloblastin exhibited an inhibitory effect on epithelial cell proliferation *in vitro* (Fig. 3). Our results suggest that ameloblastin suppresses initial periodontal destruction by inhibiting epithelial cell proliferation. Conversely, a previous study has demonstrated that ameloblastin stimulates the proliferation of human periodontal ligament cells.[25] These findings indicate that ameloblastin has differential effects on cell proliferation according to the cell type. We have no precise explanation for this phenomenon, but we speculate that the difference in viability may be because of receptor expression levels. Ameloblastin has been shown to interact with CD63,[22] although the physiological roles of this interaction remain unclear. The molecular mechanisms for the interaction between ameloblastin and CD63 are currently under investigation using mAbs established in our laboratory.

Cell growth is thought to be critically regulated by the cell cycle.[29,30] We found that ameloblastin treatment inhibited cell cycle arrest at the G1 phase (Fig. 4). The oral epithelium prevents invasion by pathogenic microorganisms and is important for periodontal wound healing. However, the down growth of epithelial cells occurs in periodontium affected by periodontitis. The presence of ameloblastin in the gingival sulcus may contribute to the prevention of down growth of the epithelium in the initiation of periodontitis. These findings show provide a valuable insight into how ameloblastin may alter epithelial turnover in the prevention of periodontal breakdown.

Funding

None.

Competing interests

None declared.

Ethical approval

Not required.

Authors contribution

Saito, Ariyoshi and Okinaga performed experiments and evaluated results. Saito and Ariyoshi contributed in drafting manuscript. Kamegawa, Matsukizono and Akebiyama were involved in preparation of the monoclonal antibody against human ameloblastin. Kitamura and Nishihara contributed in planning the study concept and performed critical revision of the manuscript.

Acknowledgement

This study was partially supported by a Grant-in-Aid for subject-solution-type development of a medical instrument from the Ministry of Economy, Trade and Industry of the Japanese government.

REFERENCES

1. Burt B. Position paper: epidemiology of periodontal diseases. *J Periodontol* 2005;76(8):1406–19.
2. Nishihara T, Koseki T. Microbial etiology of periodontitis. *Periodontol 2000* 2004;36:14–26.
3. Ready D, D'Aiuto F, Spratt DA, Suvan J, Tonetti MS, Wilson M. Disease severity associated with presence in subgingival plaque of *Porphyromonas gingivalis*, *Aggregatibacter actinomycetemcomitans*, and *Tannerella forsythia*, singly or in combination, as detected by nested multiplex PCR. *J Clin Microbiol* 2008;46(10):3380–3.
4. Rouabhia M. Interactions between host and oral commensal microorganisms are key events in health and disease status. *Can J Infect Dis* 2002;13(1):47–51.
5. Beagrie GS, Skougaard MR. Observations on the life cycle of the gingival epithelial cells of mice as revealed by autoradiography. *Acta Odontol Scand* 1962;20:15–31.
6. Dale BA. Periodontal epithelium: a newly recognized role in health and disease. *Periodontol 2000* 2002;30:70–8.
7. Dickinson BC, Moffatt CE, Hagerty D, Whitmore SE, Brown TA, Graves DT, Lamont RJ. Interaction of oral bacteria with gingival epithelial cell multilayers. *Mol Oral Microbiol* 2011;26(3):210–20.
8. Miyauchi M, Sato S, Kitagawa S, Hiraoka M, Kudo Y, Ogawa I, et al. Cytokine expression in rat molar gingival periodontal tissues after topical application of lipopolysaccharide. *Histochem Cell Biol* 2001;116(1):57–62.
9. Lee SK, Krebsbach PH, Matsuki Y, Nanci A, Yamada KM, Yamada Y. Ameloblastin expression in rat incisors and human tooth germs. *Int J Dev Biol* 1996;40(6):1141–50.
10. Krebsbach PH, Lee SK, Matsuki Y, Kozak CA, Yamada KM, Yamada Y. Full-length sequence, localization, and chromosomal mapping of ameloblastin. A novel tooth-specific gene. *J Biol Chem* 1996;271(8):4431–5.
11. Spahr A, Lyngstadaas SP, Slaby I, Pezeshki G. Ameloblastin expression during craniofacial bone formation in rats. *Eur J Oral Sci* 2006;114(6):504–11.
12. Nuñez J, Sanz M, Hoz-Rodríguez L, Zeichner-David M, Arzate H. Human cementoblasts express enamel-associated molecules in vitro and in vivo. *J Periodontal Res* 2010;45(6):809–14.
13. Hasegawa N, Kawaguchi H, Ogawa T, Uchida T, Kurihara H. Immunohistochemical characteristics of epithelial cell rests of Malassez during cementum repair. *J Periodontal Res* 2003;38(1):51–6.
14. Beyeler M, Schild C, Lutz R, Chiquet M, Trueb B. Identification of a fibronectin interaction site in the extracellular matrix protein ameloblastin. *Exp Cell Res* 2010;316(7):1202–12.
15. Sonoda A, Iwamoto T, Nakamura T, Fukumoto E, Yoshizaki K, Yamada A, et al. Critical role of heparin binding domains of ameloblastin for dental epithelium cell adhesion and ameloblastoma proliferation. *J Biol Chem* 2009;284(40):27176–84.
16. Zhang X, Diekwisch TG, Luan X. Structure and function of ameloblastin as an extracellular matrix protein: adhesion, calcium binding, and CD63 interaction in human and mouse. *Eur J Oral Sci* 2011;119(Suppl. 1):270–9.
17. Fukumoto S, Yamada A, Nonaka K, Yamada Y. Essential roles of ameloblastin in maintaining ameloblast differentiation and enamel formation. *Cells Tissues Organs* 2005;181(3–4):189–95.
18. Fukumoto S, Kiba T, Hall B, Iehara N, Nakamura T, Longenecker G, et al. Ameloblastin is a cell adhesion molecule required for maintaining the differentiation state of ameloblasts. *J Cell Biol* 2004;167(5):973–83.
19. Uchida T, Murakami C, Dohi N, Wakida K, Satoda T, Takahashi O. Synthesis, secretion, degradation, and fate of ameloblastin during the matrix formation stage of the rat incisor as shown by immunocytochemistry and immunochemistry using region-specific antibodies. *J Histochem Cytochem* 1997;45(10):1329–40.
20. Nanci A, Zalzal S, Lavoie P, Kunikata M, Chen W, Krebsbach PH, et al. Comparative immunochemical analyses of the developmental expression and distribution of ameloblastin and amelogenin in rat incisors. *J Histochem Cytochem* 1998;46(8):911–34.
21. Brookes SJ, Kirkham J, Shore RC, Wood SR, Slaby I, Robinson C. Amelin extracellular processing and aggregation during rat incisor amelogenesis. *Arch Oral Biol* 2001;46(3):201–8.
22. Iizuka S, Kudo Y, Yoshida M, Tsunematsu T, Yoshiko Y, Uchida T, et al. Ameloblastin regulates osteogenic differentiation by inhibiting Src kinase via cross talk between integrin beta1 and CD63. *Mol Cell Biol* 2011;31(4):783–92.
23. Fong CD, Cerný R, Hammarström L, Slaby I. Sequential expression of an amelin gene in mesenchymal and epithelial cells during odontogenesis in rats. *Eur J Oral Sci* 1998;106(Suppl. 1):324–30.
24. Bègue-Kirn C, Krebsbach PH, Bartlett JD, Butler WT. Dentin sialoprotein, dentin phosphoprotein, enamelysin and ameloblastin: tooth-specific molecules that are distinctively expressed during murine dental differentiation. *Eur J Oral Sci* 1998;106(5):963–70.
25. Zeichner-David M, Chen LS, Hsu Z, Reyna J, Caton J, Bringas P. Amelogenin and ameloblastin show growth-factor like activity in periodontal ligament cells. *Eur J Oral Sci* 2006;114(Suppl. 1):244–53.
26. Terpe K. Overview of tag protein fusions: from molecular and biochemical fundamentals to commercial systems. *Appl Microbiol Biotechnol* 2003;60(5):523–33.
27. Los GV, Encell LP, McDougall MG, Hartzell DD, Karassina N, Zimprich C, et al. HaloTag: a novel protein labeling technology for cell imaging and protein analysis. *ACS Chem Biol* 2008;3(6):373–82.
28. Ohana RF, Hurst R, Vidugiriene J, Slater MR, Wood KV, Urh M. HaloTag-based purification of functional human kinases from mammalian cells. *Protein Expr Purif* 2011;76(2):154–64.
29. Bartek J, Lukas J. Pathways governing G1/S transition and their response to DNA damage. *FEBS Lett* 2001;490(3):117–22.
30. O'Connor PM. Mammalian G1 and G2 phase checkpoints. *Cancer Surv* 1997;29:151–82.